# Cost effective and minimal time synthesis of mullite from a mine waste by thermal plasma process

**Swatirupa Pani, Rakesh Kumar Sahoo, Nilima Dash, Saroj Kumar Singh, Birendra Kumar Mohapatra**[*]

*Institute of Minerals and Materials Technology, Bhubaneswar 751013, India*

[*]Corresponding author. Tel: (+91) 9937350344; E-mail: bkmohapatra@immt.res.in

## ABSTRACT

The synthesis of mullite from an aluminous-rich mine waste (shale) closely associated with iron/manganese mines from Bonai-Keonjhar belt, Odisha is reported. The shale constitutes major kaolinite with minor halloysite, quartz, orthoclase and plagioclase minerals and compositionally contains 36.40 % $Al_2O_3$ and 52.10% $SiO_2$. In order to convert this mine waste to a refractory product, 'Mullite', alumina powder was added in 1:0.9; 1:1 and 1:1.1 weight ratios with the shale and thoroughly homogenized. Individual mixtures were fed in to the thermal plasma reactor and processed for only 5 minutes to form mullite. The phase and microstructure developed in the processed samples were investigated from their XRD patterns, Raman spectra and SEM images. Diagnostic peaks of the mullite phase are distinctly marked in the XRD pattern and Raman spectra of plasma treated products. Microstructure of mullite observed under SEM clearly exhibits a fused layered structure. The integrated results confirm the formation of high quality mullite from a mixture of 1:1 weight ratio. This low cost process can be implemented in industrial scale for processing of such mine waste to a value added refractory product. Copyright © 2015 VBRI press.

**Keywords:** Shaly rock; mullite; glass ceramics; alumina.

**Swatirupa Pani** is a research scholar in the Department of Hydro and Electrometallurgy in the CSIR-Institute of Minerals and Materials Technology, Bhubaneswar, India. She received her master's degree in Geology from Utkal University, Odisha. Her active areas of research interest include process mineralogy and waste utilization.

**Saroj Kumar Singh** is a chief Scientist and Head of Advanced Material Division of CSIR-Institute of Minerals and Materials Technology, Bhubaneswar, India. He has published more than 110 papers in peer reviewed journal and supervised 4 Ph.D. scholars in the field of material science

**Birendra Kumar Mohapatra** is a chief Scientist in Mineral Processing Department of CSIR-Institute of Minerals and Materials Technology, Bhubaneswar, India. He has published more than 106 papers in peer reviewed journal and supervised 10 Ph.D. scholars in the field of ore geology and waste utilization.

## Introduction

Mullite ($3Al_2O_3.2SiO_2$) is an important alumino-silicate, widely used in refractory application but rarely occurs in nature due to its high temperature and pressure formation condition. Mullite has achieved outstanding importance as refractory material due to its high melting point, little deformation under load, high shear modulus and good corrosion resistance [1, 2]. Mullite, due to its structural advantage, is the most desirable phase in alumina ceramics. Mullite exists in two stoichiometric compositions of alumina and silica i.e. 3:2 ($3Al_2O_3.2SiO_2$) and 2:1 ($2Al_2O_3.2SiO_2$) with two different structural forms i.e. orthorhombic and tetragonal. The tetragonal phase forms within the temperature range of 900 ℃ to 1300 ℃ and the stable orthorhombic phase above 1300 ℃ temperature [3]. Basically, the orthorhombic phase of mullite is used as a refractory at high temperature [3, 4]. The formation of the stoichiometric composition and phase of the mullite depends on the synthesis technique and on the kind of raw material used.

As mullite does not occur in nature, a lot of efforts are being made to prepare mullite ceramics over several decades. Several techniques like: sol-gel, hydrolysis, hydrothermal synthesis and co-precipitation [5-8] are

reported for the synthesis of mullite using high quality $SiO_2$ and $Al_2O_3$ powder as the raw materials. Recently, Zadeh et al [9] reported the synthesis of mullite nano fibers by electrospinning procedure. However, the disadvantage of these processes includes expensive starting material, low yield, higher production time and hence not suitable for large scale industrial production. The synthesis of mullite from various low-cost natural material / waste such as kaolin [10-13], silimanite [14, 15], andalusite [16, 17], bauxite, fly ash [18] and bentonite [19] has also been undertaken. But, the processing time was reported to be longer.

In this paper mullite has been synthesized from an aluminous-rich rock (termed as shale), a largely available mine waste associated with iron and manganese ore deposits in Bonai-Keonjhar belt, Odisha, India. Every time when manganese/iron ore is raised from a mine a lot of shaly rock is generated and stock piled without any use, hence considered as waste. This mine waste causes both storage and environmental problem. The effective utilisation of such voluminous shaly rock from this region would not only decrease environmental pollution but also produces high value added products.

Hence, attempt has been made in this paper to prepare mullite from an inexpensive starting material (shaly rock) in a plasma furnace that would substantially reduce the production time. However, the alumina to silica ratio in the feed material is only 1.4:2 which is far below 3:2 ratio, required for a good quality mullite formation. Hence, in order to synthesize mullite with an accurate chemical stoichimetric and appropriate microstructure, alumina powder and shaly rock in 1:0.9, 1:1 and 1:1.1 ratio was thoroughly mixed and processed in a thermal plasma reactor. After plasma processing the mullite products were analyzed using scanning electron microscope, X-ray diffraction and Raman spectroscopy to find out their quality and results are reported.

## Experimental

### Materials

Bulk white coloured shaly rock sample was collected from the mine profile of Purnapani manganese deposit (**Fig. 1**) located in Bonai-Keonjhar Belt, Odisha. High pure (99.8%) alumina powder (SRM 30) was purchased from NALCO, Bhubaneswar, India.



**Fig. 1.** Field exposure of shaly rock (the mine waste).

### Synthesis of mullite

The shale sample in different ratio such as 1:0.9, 1:1 and 1:1.1 was thoroughly mixed with high pure alumina powder. This mixed material was ball milled (PM 100 CM) for 30 minutes. This homogenized material was charged as plasma feed for the synthesis of high quality mullite. An indigenously developed 50 KW thermal plasma reactor was used for this purpose. Oxygen was used as plasma forming gas and the flow rate was kept fixed for 1lit/min. The reactor hearth is insulated with bubble alumina and kept in a water cooled chamber. High pressure cold water was allowed to flow throughout the external body of the reactor. Provisions were made for fine adjustment of the electrode distance to obtain the required arc length.

The Plasma forming gas ($O_2$) flows into the electrode space through a narrow hole of the upper electrode (cathode). The mixed raw powders of "shale and alumina" in different proportion were fed to the plasma reactor for the synthesis of mullite. The feeding powders were directly exposed to plasma for heating/melting. The different parameters of plasma processing are: 300A current, 50V voltage and time duration 5min.The schematic diagram for experimental set up is shown in **Fig. 2**. Three different compositions of white shale-alumina mixture was prepared with respect to the weight ratio of alumina and treated in a high temperature plasma furnace of 50 KW power for 5 minutes duration. The details of the mullite feed and plasma time is mentioned in **Table 1**.
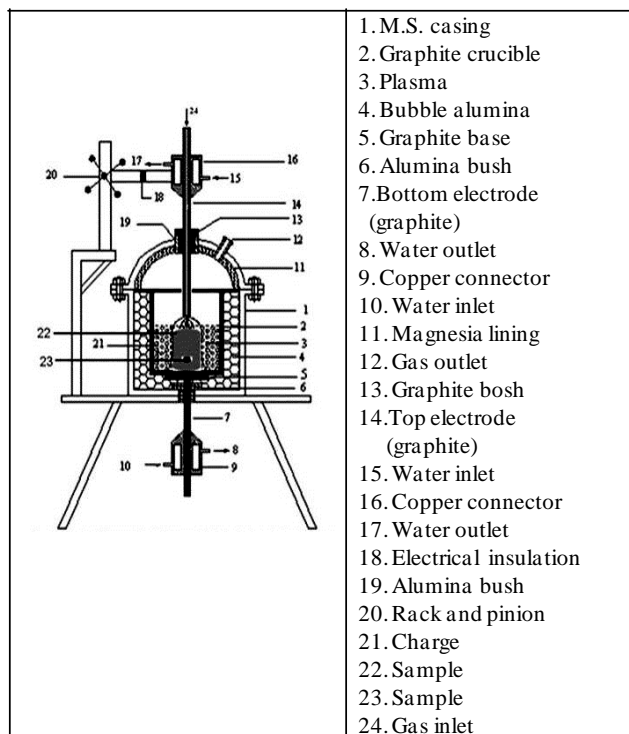


1. M.S. casing
2. Graphite crucible
3. Plasma
4. Bubble alumina
5. Graphite base
6. Alumina bush
7. Bottom electrode (graphite)
8. Water outlet
9. Copper connector
10. Water inlet
11. Magnesia lining
12. Gas outlet
13. Graphite bosh
14. Top electrode (graphite)
15. Water inlet
16. Copper connector
17. Water outlet
18. Electrical insulation
19. Alumina bush
20. Rack and pinion
21. Charge
22. Sample
23. Sample
24. Gas inlet

**Fig. 2.** Schematic diagram of plasma furnace holder.

### Characterisation techniques of feed and product

A part of the feed (shaly rock) and product (fused mullite) sample was powdered for XRD study (Philips-PW-1700) and polished surface was prepared for SEM study (JEOL, JSM-6510).The compositional analysis of feed shale

sample was carried out using Philips X-ray fluorescence spectrometry (PW-1400). Micro Raman measurements of both feed and product were carried out at room temperature using Renishaw inVia instrument in a back scattering geometry. An Ar-ion laser with 514 nm wavelength was used as an excitation source. The Raman spectrometer was equipped with double subtractive monochromator with a 1,800 grooves/mm holographic grating and a Peltier-cooled CCD detector.

**Table 1.** Wt % of Shale alumina mixture and duration of heat treatment.

| Sample code | Shale (in gm) | Alumina (in gm) | Plasma time (in min) |
|---|---|---|---|
| 1 | 100 | 90 | 5 |
| 2 | 100 | 100 | 5 |
| 3 | 100 | 110 | 5 |

## Results and discussion

### Characterization of shale, the mine waste

The shale sample was characterized in respect of their physical, mineralogical and chemical properties. The shale is white in colour, fine grained and around 99% is below 0.01mm in size. The size classification results of the shale sample are shown in **Table 2**.

**Table 2.** Size distribution (wt %) in bulk shale sample.

| Size (in mm) | Wt % |
|---|---|
| -1+0.5 | 0.3 |
| -0.5+0.25 | 0.4 |
| -0.25+0.1 | 0.4 |
| -0.1 | 98.9 |

The grain density of this sample is found to be 2.27. The electron micrographs of bulk shale sample are shown in **Fig. 3**. As can be observed, the grains generally appear flaky, though same prismatic and irregular grains are also observed.
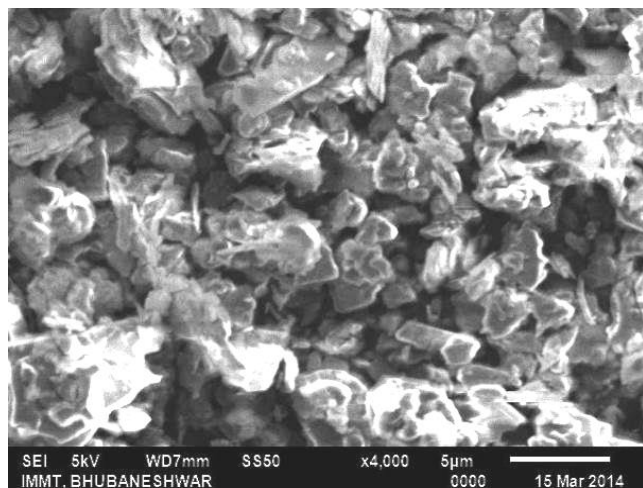


**Fig. 3.** Electron micrographs of shale sample.

Powdered shale sample was subjected to X-ray diffraction study and the result is shown in **Fig. 4a**. It essentially constitutes silicate minerals like kaolinite [$Al_4Si_4O_{10}(OH)_8$] and halloysite [$(Al_4Si_4)O_{10}(OH)_8 \cdot 8H_2O$] with minor orthoclase ($KAlSi_3O_8$), plagioclase ($NaAlSi_3O_8$) and quartz ($SiO_2$). The chemical analysis results of shale sample are given in **Table 3**. As it is seen, the shale is free from Mn, though located in a manganese mine, has negligible iron and contains appreciable amount of alumina and silica. From the analysis result (**Table 3**), it is apparent that the white shale sample has not the optimal stoichiometric ratio of $Al_2O_3:SiO_2$ as it is required for mullite ($3Al_2O_3 \cdot 2SiO_2$). Hence, additional alumina in different percentage was added to the white shale to find out at what ratio homogenous growth of mullite takes place in the sample.
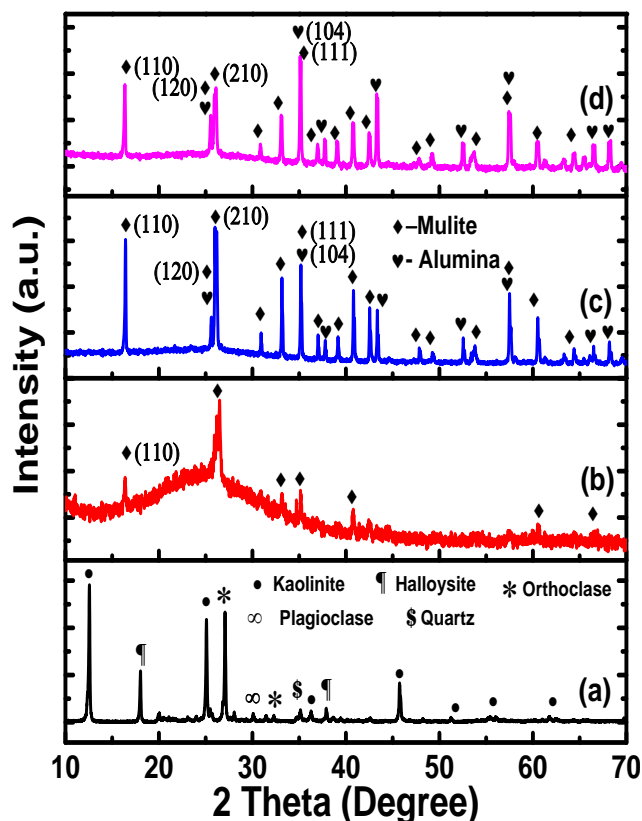


**Fig. 4.** Comparative XRD patterns of (a) white shell, (b) Sample-1, (c) Sample-2, (d) Sample-3.

**Table 3.** Distribution pattern of major and minor elements (in wt %) in the shale sample.

| Mn | Fe | $Al_2O_3$ | $SiO_2$ | $P_2O_5$ | LOI |
|---|---|---|---|---|---|
| - | 0.75 | 36.40 | 52.10 | 0.01 | 10.09 |

### Characterisation of mullite

This shale was mixed with different weight ratio of alumina and plasma processed. The shale: alumina mixed ratios was mentioned in Table 4. After mullatilization the grain density of the three samples were determined (**Table 4**). Density of 1:1 ratio of shale: alumina matches with the

theoretical data. The three mullite products, so obtained were characterized in respect of microstructure and other properties.

**Table 4.** Grain density of mullite at different Alumina percentages.

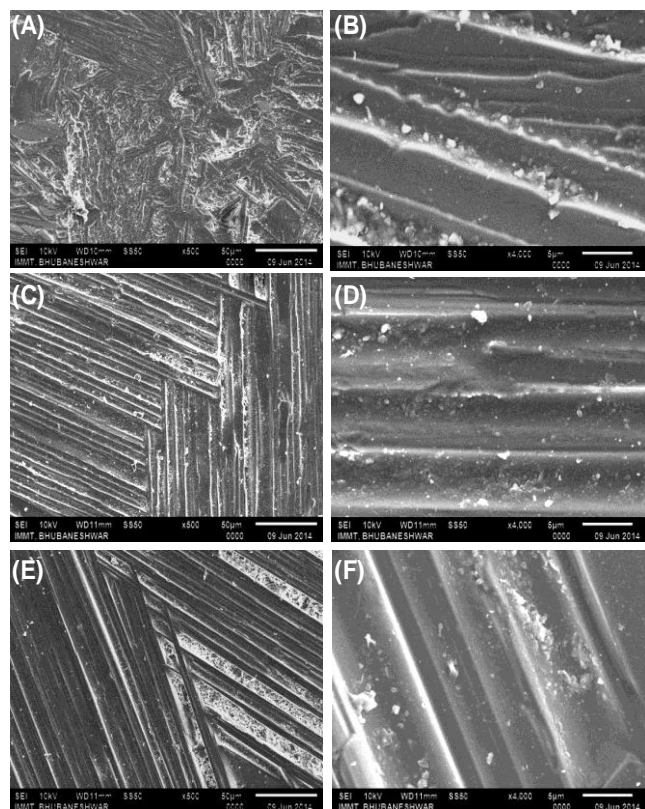| Sample code | Shale : alumina | Grain Density |
|---|---|---|
| 1 | 1 : 0.9 | 2.85 |
| 2 | 1:1 | 3.12 |
| 3 | 1:1.1 | 3.39 |

**Fig. 5**. SEM image of mullite at different alumina composition A & B: sample -1; C & D: Sample -2; E & F: Sample -3.

*XRD findings*

XRD pattern of the feed shale sample is compared with mullite (**Fig. 4**). In the former sample several phases like: kaolinite, halloysite, orthoclase, plagioclase and quartz are observed. However, after plasma processing, several changes in the XRD patterns are observed. In Sample-1 (by taking 1:09 of shale: alumina weight ratio), the major phase of mullite is in the form of $Al_6Si_2O_{13}$ which matches with the JCPDS#15-0776. The hump like shape in the background at 26.1° (which is the major peak of mullite) indicates the amorphous mullite phase formation at this composition. By increasing the alumina shale ratio to 1:1 in the plasma feed (sample-2), a crystalline phase of mullite with crystal structure of $Al_6Si_2O_{13}$, matching with JCPDS#15-0776 (**Fig. 4c**), and a secondary minor phase of alumina (JCPDS#03-0513) is recorded.

Further increase of alumina in the charge mix (1:1.1 ratio) also results in the development of mullite phase but an additional prominent phase of corundum (JCPDS#03-0513) appears (**Fig. 4d**). In this case, the primary peak of the alumina at 35.1° (d = 2.5 Å) is more intense than the primary mullite peak observed at 26.1° (d = 3.4 Å) which indicates the presence of crystalline alumina residue along with mullite in the final product. However, reverse is the case when alumina is added at 1:0.9 ratio with the shale before plasma processing.

Thus, addition of alumina with shale at 1:0.9 ratio, initiates the amorphous mullite phase formation, while increasing the ratio to 1:1 gives the desired crystalline mullite with minor alumina phase.

Further, increase in the ratio to 1:1.1 leaves behind the residual corundum phase with mullite.

Moreover, this study implies that, the white shale promote the mullite formation at high temperature plasma treatment. The formation of the bulk mullite from the shale powder follows the steps of bulk decomposition of the shale at high temperature plasma in oxygen atmosphere followed by diffusion of the additional alumina powder and formation of low viscosity liquid intermediate phase. Finally, the intermediate liquid phase creates the mullite bonding between the $SiO_2$ and $Al_2O_3$. Here, the oxygen plasma plays a vital role in decomposition of the shale. Oxygen promotes both the surface and bulk diffusion of the alumina powder to form the intermediate liquid. However, mixing a optimum amount of the alumina to the shale before plasma processing plays a significant role in formation of the highly crystalline mullite without any additional impurity phase after plasma processing.

*SEM findings*

The microstructure of the Sample-1 is shown in **Fig. 5a** & **5b**. The microstructure of the surface is irregular and fibres are very sort and ill developed (**Fig. 5a**). Some small spinel grains (glassy phase) are also seen at lower magnification.

Higher magnification image shows crenulated and irregular outline of the fibres (**Fig. 5b**). Set of fibres appear merging with other at acute angles.

In contrast, Sample-2 shows presence of large well developed mullite whiskers at different orientation (**Fig. 5c**). These fibres appear compact and massive at higher magnification (**Fig. 5d**). The as-grown fibers are regular and a particular set of fibers inter lock with other sets at an obtuse angle. In Sample-3, the mullite whiskers are more developed in comparisons to that of Sample-2 (**Fig. 5e**). But, due to addition of extra alumina some corundum grains are observed above the mullite fibres at higher magnification (**Fig. 5f**). Moreover, Sample-2 shows well developed compact microstructure in comparisons to the rest two cases.

Thus, the above microstructures indicated the effect of optimal alumina addition to shale matrix. *Yugeswaran et al.* [20] reported that the oxides like $B_2O_3$, $TiO_2$, etc. play important role in promoting the growth of mullite grains. The optimal addition of the above oxides during the synthesis of mullite alters the viscosity of the plasma feed. Basically, the oxides reduce the glass viscosity of the smelted product and enhance the mobility of the diffusing species. In present work, addition of alumina plays the dual role: as an oxide additive and the filler which give strength to the mullite matrix during the process of smelting. However, the addition of insufficient amount of the alumina with shale forms the ill developed and less compact fibers

while excess addition of alumina leaves behind the corundum precipitates.

*Raman spectroscopic findings*

The major phase formation in these plasma processed samples was observed from the X-ray diffraction patterns which indicated the variation in the compositions of the prepared mullites. But, the minor change in this chemical composition cannot be verified by the chemical analysis because of the presence of the glassy matrix [21]. Hence, Raman analyses of all three mullite samples were carried out to confirm the presence of mullite phase. A comparative Raman spectrum of the feed shale and three mullite samples after processing is shown in **Fig. 5**.
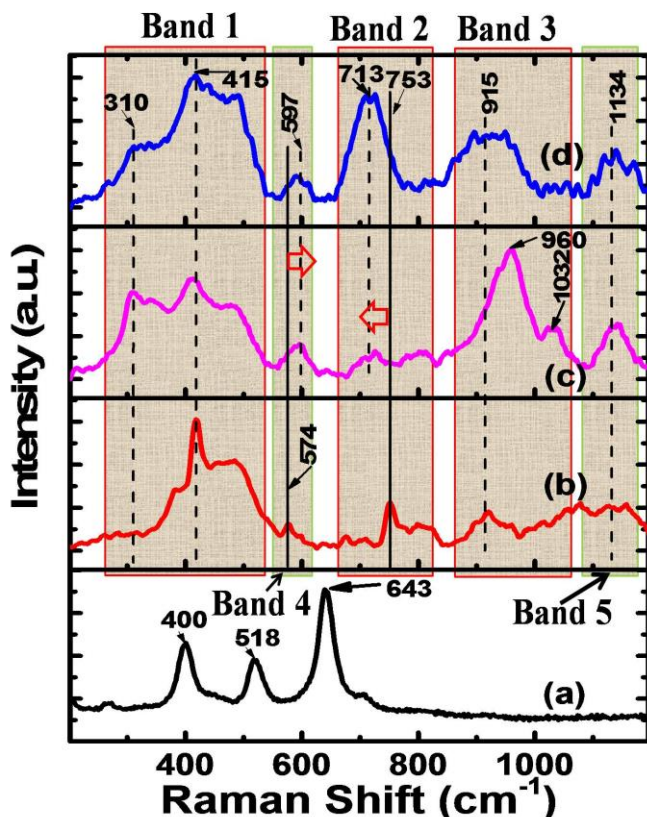


**Fig. 5.** Comparative Raman spectra of: shale, (a, b) mullite [sample-1], (c) mullite [sample-2] and (d) mullite [sample-3].

The Raman spectrum of feed shale sample (**Fig. 5a**) consists of three major bands at 400, 518 and 643 cm$^{-1}$. The Raman peak at 400 cm$^{-1}$ corresponds to the orthoclase or plagioclase family whereas the peaks at 518 cm$^{-1}$ and 643 cm$^{-1}$ correspond to the halloysite and kaolinite type of clays [22]. **Figs. 5b**, **5c** and **5d** show the Raman spectra of the three mullite samples. These spectra are very broad asymmetric in nature. These types of broad bands are usually observed for crystals with vacancy structure [21, 23]. These spectra of mullite samples consist of three major bands in the range of 249-537, 655-785 and 842-1040 cm$^{-1}$ and two minor bands in the range of 537-613 cm$^{-1}$ and 1086-1191 cm$^{-1}$.

The first major band (249-537 cm$^{-1}$) consists of one central peak at 415 cm$^{-1}$ and two shoulders at 488 and 310 cm$^{-1}$. The shoulder at 310 cm$^{-1}$ was observed in sample-2 and sample-3 but absent in sample-1. The peaks at 310 and 415 cm$^{-1}$ are attributed to the bending mode of 6 member Si-O-Al rings [24-27].

The second major Raman band observed in between 655-785 cm$^{-1}$ was related to the alumina content in the sample [23]. Interestingly, this band centre was appeared to shift towards lower frequency side (shown by arrow mark towards left) and also the band gradually gets prominent as the alumina content in the plasma feed increases. The band centre for this band was observed at 753, 726 and 713 cm$^{-1}$ for sample 1, 2 and 3, respectively. The doublet at 713 cm$^{-1}$ and 753 cm$^{-1}$ for sample-3 indicated the presence of separate corundum phase in the mullite matrix in comparisons to sample-1 and sample-2.

The third major Raman band (842-1040 cm$^{-1}$) was observed for all mullite samples. This band consists of one central peak at 915 cm$^{-1}$ and a shoulder at 1032 cm$^{-1}$. The bands at 960 and 1032 cm-1 are ascribed to T-O (T = Si or Al) stretching motion of Si-O-Al. The shoulder at 1032 cm$^{-1}$ was observed only in sample-2 and absent in sample-1 and sample-3. This band (842-1040 cm$^{-1}$) was more intense for sample-2 and the centre of this band was observed at 960 cm$^{-1}$. This band was shifted by 45 cm$^{-1}$ towards higher frequency side with respect to sample-1 and sample-3. This shift in peak centre towards the higher frequency side and the increase in prominence of this band indicated the superior phase formation in sample-2 in comparison to sample-1 and sample-3.

The first minor band (band 4: 537-613 cm$^{-1}$) corresponds to the amorphous alumino-silicates containing mainly 4-membered rings and this band shift toward the higher frequency side as the alumina content in the feed increases (shown by arrow mark towards right). The second minor band (Band 5: 1086-1191 cm$^{-1}$) is attributed to the asymmetric stretching modes of T-O for alumino-silicates [27].

## Conclusion

The conclusions made from the foregoing results are as follows:

i) An aluminous rich rock (shale), associated with iron and manganese ore occurs in large volume in Bonai-Keonjhar belt, Odisha but do not find any use and hence considered as waste.

ii) The shale contains kaolinite, halloysite, feldspar minerals and composed of 36% of alumina & 52% of silica and almost devoid of Mn / Fe impurities.

iii) Such a mine waste was converted to mullite a value added product for refractory application.

iv) For mullite preparation, shale was thoroughly mixed with three different proportion of alumina such as 1:0.9, 1:1 and 1:1.1 and subjected to heat treatment in a plasma furnace.

v) The product was examined under SEM, XRD and Raman spectroscopy.

vi) The shale: alumina mixed in 1:1 proportion was found to produce homogenous single phase growth of mullite which was confirmed from the XRD data and corroborated by Raman spectroscopy.

vii) By adding low percentage of alumina with shale (1:0.9), in addition to mullite, spinel phase appears in the product, while by adding more alumina (1:1.1) in shale, besides mullite, corundum appears. This finding

was also confirmed from their XRD and Raman spectral patterns. The morphological change and the formation of the corundum phase were observed from the SEM images.

The above study thus demonstrated that an inexpensive waste material can be converted to a usable product through plasma processing method which is very competitive to conventional sintering as the processing time is very less and hence would be cost effective. Further, these findings have opened up avenue for initiation of pilot scale study to convert such mine waste to wealth.

## Reference

1. Ohira, H.; Ismail, M.G.; Yamomoto, Y.; Akibaa, T.; Sōrniyab, S.; *J. Eur. Ceram.Soc.* **1996**, *16*, 225.
   **DOI:** 10.1016/0955-2219(95)00155-7
2. Zaki, Z.I.; Mostafa, Nasser Y.; Ahmed, Y.M.Z.; *Int. J. of Ref. Metals and Hard Materials* **2014**, *45*, 23.
   **DOI:** 10.1016/j.ijrmhm.2014.03.006
3. Schneider, H.; Komareni, S.; Mullite, WILEY-VCH Verlag GmbH & Co.KGaA, Weinheim, **2005**.
4. Moallemi Nejad, M.; Heshmati Manesh, S.; Ataie, A.; *Int. J. Modern Phys.B.* **2008**, *22*, 2947.
   **DOI:** 10.1142/S0217979208047791
5. Gesing, T. M. R.; Fischer, X.; Burianek, M.; Mühlberg, M.; Debnath, T.; Rüscher, C. H.; Ottinger, J.; Buhl, J.C.; Schneider, H.; *J. Eur. Ceram.Soc.* **2011**, *31*, 3062.
   **DOI:** 10.1016/j.jeurceramsoc.2011.04.004
6. Viswabaskaran,V.; Gnanam, F.D.; Basubramanian, B.; *Ceram. Int.* **2002**, *28*, 557.
   **DOI:** 10.1016/S0272-8842(02)00010-X
7. Chen,Y. F.; Wang, M.C.; Hon, M.H.; *J. Eur. Ceram. Soc.* **2004**, *24*, 2389.
   **DOI:** 10.1016/S0955-2219(03)00631-9
8. Pei-Ching Yu, Yung-Wei Tsai, Fu-Su Yen, and Cheng-Liang Huang, *J. Am. Ceram. Soc.* **2014**, *8*, 2431.
   **DOI:** 10.1111/jace.12989
9. Zadeh, M.M.A.; Rad, M.K.; Ebadzadeh, T.; *Ceram. Int.* **2013**, *39*, 9079**.**
   **ISSN:** 02728842
10. Chen, C.Y.; Lan, G.S.; Tuan, W.H.; *J. Eur. Ceram. Soc.* **2000**, *20*, 2519.
    **DOI:** 10.1016/S0955-2219(00)00125-4
11. Kim, Y.-W.; Kim, H.D.; Park, C.B.; *J. Am. Ceram. Soc.* **2005**,*88*, 3311.
    **DOI:** 10.1111/j.1551-2916.2005.00597.x
12. Sainz, M. A.; Serrano, F. J.; Amigo, J. M.; Bastida, J.; Caballero, A.; *J. Eur. Ceram. Soc*. **2000**, *20*, 403.
    **DOI:** 10.1016/S0955-2219(99)00183-1
13. Temuujin, J.; MacKenzie, K.J.D.; Schmucker, M.; Schneider, H.; McManus, J.; Wimperis, S.; *J. Eur. Ceram. Soc.* **2000**, *20*, 413.
    **DOI:** 10.1016/S0955-2219(99)00188-0
14. Rahman, S.; Feustel, U.; Freimann, S.; *J. Eur. Ceram. Soc.* **2001**, *21*, 2471.
    **DOI:** 10.1016/S0955-2219(01)00386-7
15. Rüscher, C. H.; *J. Eur. Cer. Soc.* **2001**, *21*, 2463.
    **DOI:** 10.1016/S0955-2219(01)00264-3
16. Bouchetou, M. L.; Ildefonse, J. P.; Poirier, J.; Daniellou, P.; *Ceram. Int.* **2005**, *31*, 999.
    **DOI:** 10.1016/j.ceramint.2004.10.015
17. Mazel, F.; Gonon, M.; Fantozzi, G.; *J. Eur. Cer. Soc.* **2002**, *22*, 453.
    **DOI:** 10.1016/S0955-2219(01)00315-6
18. Dong, Y.; Feng, Xy.; Feng, Xe.; Ding, Y.; Liu, X.; Meng, G. ; *J. Alloys Compd.* **2008**, *460*, 599.
    **DOI:** 10.1016/j.jallcom.2007.06.023
19. Santana, L.N.L.; Gomes, J.; Neves, G.A.; Lira, H.L.; Menezes, R.R.; Segadaes, A.M.; *Appl. Clay Sci.* **2014,** *87, 28.
    **DOI:** 10.1016/j.clay.2013.11.018
20. Yugeswaran, S.; Selvarajan, V.; Lusvarghi, L.; Karoly, Z.; Szepvolgyi, J.; *Mater. Manuf. Processes* **2011**, *26*, 813.
    **DOI:** 10.1080/10426914.2010.508805
21. Mcmillan, P.; Piriou, B.; *J. Non-Cryst. Solids.* **1982**, *53*, 279.
    **DOI:** 10.1016/0022-3093(82)90086-2
22. Frost, R. L.; *Clays & Clay Miner.* **1995**, *43*, 191.
    **DOI:** 10.1346/CCMN.1995.0430206
23. 23. Keramidas, V.B.; White, W.; *J. Phys. Chem. Solid* **1973**, *34*, 1873.
    **DOI:** 10.1016/S0022-3697(73)80108-8
24. Dutta, P.K.; Shieh, D.C.; Puri, M.; *J. Phys. Chem.* **1987**, *91*, 2332.
    **DOI:** 10.1021/j100293a025
25. Griffith,W.P.; *J. Chem. Sco.* **1969**, *A9*, 1372.
    **DOI:** 10.1039/J19690001372
26. Macmillan, P.; *Am. Mineral.* **1984**, *69*, 622.
27. Guang Xiong, Yi Yu.; Feng-Shou Xiao, Can Li.; *Microporous Mesoporous Mater.* **2001**, *46*, 23.
    **DOI:** 10.1016/S1387-1811(01)00271-2